

Hadron spectroscopy in a flux-tube quark model

J. Carlson, J. B. Kogut, and V. R. Pandharipande

Department of Physics, University of Illinois at Urbana-Champaign, 1110 West Green Street, Urbana, Illinois 61801

(Received 13 June 1983)

Color-magnetic interactions (one-gluon exchange) are incorporated into a semirelativistic quark model and the spectra of ground states and orbital and radial excitations of light mesons, light baryons, charmonium, and b -quarkonium are calculated by treating the magnetic splitting exactly by variational methods. The π - ρ splitting is fit and the N - Δ splitting is predicted in excellent agreement with experiment. In general, spin-spin and tensor splittings among light mesons and light baryons are calculated in good agreement with experiment. The splittings in heavy-meson spectroscopy are also predicted accurately, including the P -wave states of charmonium and b -quarkonium. Some problems and limitations of the quark-model description of the light mesons and baryons are emphasized. Spin-orbit splittings in the light mesons and P -wave baryon multiplets are calculated, but a unified understanding of the systematics is not obtained. Radial excitations in the meson and baryon systems are generally in error by 100–150 MeV, and the systematics are not understood.

I. INTRODUCTION:

SUMMARY OF PUZZLES AND RESULTS

We have recently proposed¹ (Ref. 1 is denoted henceforth by I) a semi-relativistic quark model of mesons and baryons based on quantum chromodynamics (QCD). An initial investigation into the spectrum of the model has encouraged us to pursue it in greater depth and see whether it can predict and/or accommodate the hadron spectrum. This paper presents the results of our efforts. We will discuss both the spectra of light and heavy quarks and will compute energy levels of ground states and orbital and radial excitations. The spin-spin, tensor, and spin-orbit splittings of light mesons and baryons will be discussed in some detail. A large number of calculations will be presented. Our general view of the results is that the quark model in general and the model of this paper in particular confront the data quite well. However, it is not the purpose of this paper to advertise the successes of the quark model—we are just as interested in delineating its puzzles and failures to, in the long run, better understand the underlying theory of the strong interactions.

An important step toward placing the constituent quark model on a more interesting, fundamental level comes from the work of De Rújula, Georgi, and Glashow,² who proposed that the splittings within the hadronic multiplets could be estimated on the basis of short-distance, single-gluon-exchange graphs of SU(3) Yang-Mills gauge theory. The long-distance features of the potential could be abstracted from models of confinement or lattice gauge theory, and a comprehensive study of the spectrum could be attempted. This was initiated in Ref. 2 and was taken up more systematically by Isgur and Karl.³ We will continue this line of thinking using our SU(3) interacting-string-model potential for mesons and baryons introduced in I. We will use the spin-independent potential as given in that article to represent the color-electric interactions, and not fine-tune it to all the data we consider here. Our

emphasis instead will be on the splittings caused by color-magnetic interactions.

We should summarize some of the major physics issues of interest to us before discussing the technical details of the model. A long-standing problem with the quark model is its description of the pion. In QCD the pion is believed to be a massless Goldstone boson which results from the spontaneous breakdown of chiral symmetry. Its mass of 140 MeV is believed to arise simply from the small bare masses of the u and d “light” quarks which explicitly break the continuous chiral symmetry of the model. One consequence of the symmetry breakdown is the generation of a dynamical quark mass. This dynamical mass is presumably the quark used in constituent models of the hadron spectrum. These models are, however, very crude and do not bear a clear relationship to the spontaneous symmetry breaking underlying them—they typically describe the light mesons with a quark-antiquark ($q\bar{q}$) wave equation similar to or identical with the Schrödinger equation. Then the Goldstone nature of the pion is completely obscured and questions arise as to whether a two-quark picture of the pion is fundamentally wrong, etc. Here we shall argue that the quark-model description of the pion is not such a disaster. The elements in our resolution of this problem are (1) the spin-spin interaction induced by single-gluon exchange, and (2) a nonperturbative, variational treatment of the π - ρ and N - Δ splittings.

The spin-spin potential induced by single-gluon exchange between static quarks is

$$V_{SS} = \frac{4}{3} \alpha_c \frac{2\pi}{3m^2} \vec{\sigma}_q \cdot \vec{\sigma}_{\bar{q}} \delta(\vec{r}), \quad (1.1)$$

α_c is the strong-interaction (color) fine-structure constant, m is the constituent quark mass, and $\vec{\sigma}$ is the Pauli matrix describing the spin of the static quark. In the absence of this spin-spin interaction the pion and ρ are degenerate. The potential V_{SS} provides a natural way of splitting the π

down toward zero mass and the ρ up to its experimental value of 770 MeV. In first-order perturbation theory, V_{SS} shifts the spin-zero pion 3 times as much as it shifts the spin-one ρ , so this approach has some promise. It is equally clear, however, that first-order perturbation theory is completely unjustified here since the induced splitting is comparable to the energy of the zeroth-order level. To deal with this we must treat the spin-spin forces of QCD more accurately. To pursue this idea in a completely justifiable manner, one might simply abandon the potential picture which motivated the problem and calculate single-gluon exchange and its non-Abelian radiative corrections to higher orders retaining quark-recoil effects, etc. using the full perturbative apparatus of QCD. This is beyond our sights and our approach will be more modest, intuitive, and model dependent. We will carry out variational calculations and compute the effects of the V_{SS} exactly in the context of our semirelativistic wave equation. To do this we imagine that higher-order Feynman graphs decorating the single-gluon exchange between quarks smear the color charges of the quarks over a small space-time region and effectively regulate the singular δ function in Eq. (1.1). We replace the pointlike quark-gluon vertex with a form factor $\exp(-\frac{1}{2}\Lambda^2 \vec{q}^2)$, where Λ is the “size of the quark” and \vec{q}^2 is the momentum transfer between them. Now the spin-spin potential can be treated variationally and Λ can be fixed by the π - ρ splitting. In the text we shall see that this is easy to do with sensible values for Λ and the conventional value for the strong-interaction fine-structure constant $\alpha_c \cong 0.375$ and constituent quark masses $m \approx 360$ MeV. This exercise becomes more interesting when we next address other spin-spin splittings in the light-meson, light-baryon sector of the theory. Using our baryon wave equation, we calculate the N - Δ splitting and find excellent agreement with experiment. Other spin-spin splittings are also predicted successfully. This amusing result suggests that although our quark model does not have chiral symmetry it is not far from the truth.

Single-gluon exchange also predicts a tensor force:

$$V_T = \frac{4}{3}\alpha_c \frac{1}{4m^2} \frac{1}{r^3} S_{q\bar{q}}, \quad (1.2)$$

$$S_{q\bar{q}} = \frac{3}{r^2} \vec{\sigma}_q \cdot \vec{r} \vec{\sigma}_{\bar{q}} \cdot \vec{r} - \vec{\sigma}_q \cdot \vec{\sigma}_{\bar{q}}. \quad (1.3)$$

The $\exp(-\frac{1}{2}\Lambda^2 q^2)$ form factors remove the $1/r^3$ singularity, and the resulting V_T can be treated exactly in a wave equation. We do this and find good evidence for the one-gluon-exchange tensor interaction in meson and baryon spectra.

And finally, one-gluon exchange also predicts the spin-orbit interaction:

$$V_{SO} = \frac{4}{3}\alpha_c \frac{1.5}{m^2} \frac{1}{r^3} \vec{L} \cdot \vec{S}. \quad (1.4)$$

The r^{-3} singularity is removed by the form factors, and Eq. (1.4) can then be used with some success to study the spectra of heavy mesons. This interaction, however, is not suitable for light mesons and baryons where $\langle |p| \rangle \gtrsim m$.

Recalling the classical derivation of spin-orbit forces, one of the m^{-1} factors in (1.4) comes from the replacement $\vec{v} \rightarrow \vec{p}/m$, and the other from the Dirac magnetic moment. Clearly $\vec{v} \rightarrow \vec{p}/m$ is not a sensible replacement for light quarks. We propose instead $\vec{v} \rightarrow \vec{p}/\langle (m^2 + \vec{p}^2)^{1/2} \rangle$ as a natural way to treat the kinematics more relativistically. So, in our calculations of light mesons and baryons we multiply V_{SO} by

$$\frac{m}{\langle (\vec{p}^2 + m^2)^{1/2} \rangle} x, \quad (1.5)$$

where the expectation value $\langle \dots \rangle$ is over the hadron wave function, and x is a dimensionless parameter chosen to fit the spectra. We obtain a reasonable description of spin-orbit splitting in light mesons with $x \approx 0.7$ (e.g., the A_2 - A_1 - δ splitting which is caused by V_T and V_{SO} will be accurately reproduced). However, it is well known³ that the P -wave baryon spectrum has little spin-orbit splitting, and is best explained with $x=0$. Our calculations confirm this. With $x=0.7$, the P -wave baryon theoretical and experimental spectra would disagree significantly.

What could be the resolution of the spin-orbit debacle? Coupling to the pion cloud has been suggested.⁴ Interference of the conventional spin-orbit splitting from single-gluon exchange at short distances with an opposite-sign spin-orbit splitting of a long-distance *scalar* confining potential has also been suggested.³ These proposals are not very convincing in light of the strong difference between meson and baryon splitting patterns. The second suggestion would require mesons to be smaller than baryons so that the cancellation could occur in the baryons but not the mesons. Baryons are in fact somewhat larger than mesons in general, but this is not a large effect so the argument seems quite tenuous and unnatural. Perhaps the three-body character of the baryon wave function plays an essential role in the resolution. We emphasize that this is an important spectroscopic puzzle; we do not have a solution but we urge further study of it.

Although we emphasize energy levels in this article, our calculations also yield variational wave functions for the states. One interesting feature of them is their small radii. In this model the pion has a radius of $R_{\text{rms}}=0.16$ fm and the nucleon has $R_{\text{rms}}=0.32$ fm. These are much smaller than the experimental charge radii of these hadrons of 0.55 and 0.90 fm, respectively, measured in peripheral scattering experiments. The calculated pion is particularly small because of the attractive spin-spin force which is responsible for its small mass. One interpretation of the difference between the theoretical and experimental radii is that they refer to different features of the states—the theoretical calculation gives the size of the valence-quark distribution while the experimental value reflects the pion clouds surrounding the valence quarks. It may be that the small valence-quark radii predicted here do, in fact, have some experimental support. The mean kinetic energy of the valence quarks in this model’s nucleon is approximately 600 MeV. A value of this order is preferred by the Feynman, Field, and Fox⁵ analysis of large-transverse-momentum hadronic scattering processes.

Our potential model is very simple to apply to the cal-

ulation of excited meson and baryon states. In this application it is clearly superior to other models such as the MIT bag model. In the text we consider orbital and radial excitations in detail. The agreement with experiment⁶ is in general quite good, although 10% errors are found in some cases. Radial excitations are particularly interesting. The Roper resonance, the first radial excitation of the nucleon, lies at 1440 ± 40 MeV. Harmonic-oscillator quark models have always overestimated its mass by several hundred MeV. This can be interpreted as indicating that the harmonic-oscillator potential increases too rapidly as the interquark distance grows. Our linear-confinement model also overestimates the mass of the Roper, but the disagreement with experiment is only 130 MeV. This error would suggest that the linear confinement potential is also too steep, but this may not be the true resolution of this problem because the systematics of the meson radial excitations are different.

The first radial excitation of the pion, the π' lies at 1300 ± 100 MeV and our model gives 1110 MeV. The mass of the first radial excitation of the ρ , the ρ' , is controversial. It may lie at ~ 1250 MeV in which case our prediction of 1450 MeV is high, or it may be 1600 ± 20 MeV. The experimental situation will have to be clarified before we can learn more. If 1600 MeV is the correct result, then we face the curious situation of predicting radial excitations of the mesons below their experimental values and baryons above their experimental values. The resolution of this discrepancy is not known to us. There are various suggestions in the literature of a speculative character to shift the Roper below its quark model value.

In summary, light-quark spectroscopy of spin-spin and tensor splittings are well described by a single-gluon-exchange potential in our nonperturbative potential model. This suggests that more fundamental, short-distance QCD calculations be attempted to obtain a fully consistent account of this area of spectroscopy. The case for spin-orbit splitting is not so clear.

We have also applied our model to heavy-quark spectroscopy. The α_c and the form-factor parameter Λ are varied to fit the splitting of the S - and P -wave states. Here the potential model should work better because the quark motion is less relativistic. We expect and find that the nonrelativistic limit of the gluon spin-orbit force [Eq. (1.4)] is able to explain the data. A particularly satisfactory result of the model is its description of the splittings among the P -wave states of the $c\bar{c}$ and $b\bar{b}$ mesons. If one uses the single-gluon potential given by Eqs. (1.1)–(1.4) in first-order perturbation theory, then one finds the splitting parameter r ,

$$r = \frac{m(^3P_2) - m(^3P_1)}{m(^3P_1) - m(^3P_0)} = 0.8, \quad (1.6)$$

which is in clear disagreement with the experimental charmonium results⁶ $r = 0.50 \pm 0.10$. In our nonperturbative approach the shift of the 3P_0 $c\bar{c}$ state is enhanced considerably beyond the perturbative estimate, and our calculated value of $r = 0.6$ is in good agreement with the data. Other theoretical approaches to this problem have either failed, or have fit the data assuming a scalar confining po-

tential and arguing that it contributes a “wrong-sign” spin-orbit splitting which interferes with the first-order perturbative single-gluon splitting to nearly accommodate the data. The relative simplicity of our calculation of r is very pleasing. Moreover, a similar nonperturbative shift of the $q\bar{q}$ 3P_0 state explains the energy of the δ meson. Our P -wave splittings for the $n=1$ and $n=2$ states of $b\bar{b}$ are also successful.

It is interesting to summarize the systematic variation of the parameters α_c and Λ as we turn from light mesons composed of u and d quarks (constituent mass ≈ 360 MeV) to charmonium ($m_c = 1.84$ GeV) and to b -quarkonium ($m_b = 5.17$ GeV). Our fits to the spectra use the values

$\frac{4}{3}\alpha_c$	Λ (fm)	Quark
0.50	0.13	u, d
0.50	0.05	c
0.42	0.02	b

(1.7)

The trend of α_c to decrease from 0.50 to 0.42 is consistent with asymptotic freedom. Asymptotic freedom states that the running coupling constant at an interquark distance r_b is related to that at r_c by

$$\alpha_c(r_b) = \frac{\alpha_c(r_c)}{1 + \frac{25}{12\pi}\alpha_c(r_c)\ln(r_c/r_b)^2} \quad (1.8)$$

and that the spin-independent $q\bar{q}$ potential is $-4\alpha_c(r)/3r$ at short distances. In our spectrum calculations we proceed more crudely and simply fit different constant α_c values to the light, $c\bar{c}$, and $b\bar{b}$ mesons, respectively. The relevance of asymptotic freedom can be checked by computing the relative sizes of ground states of light, $c\bar{c}$, and $b\bar{b}$ states, substituting into Eq. (1.8) and verifying that the variation of α_c with size scale agrees with the phenomenological fit. The agreement is good. The variation of Λ with quark mass m is also physically reasonable. Λ is expected to decrease as m increases by a Heisenberg uncertainty relation argument, an inspection of Feynman graphs, etc. The absolute sizes of the Λ cutoff parameters are also reasonable as compared, say, to the sizes of the meson bound states in each case. The only aspect of heavy-quark spectroscopy which is very sensitive to the Λ cutoff parameter is the position of the $nlsj^{\pi} = 0000^-$ states. Since this state is not yet experimentally observed in the $b\bar{b}$ system, our value of Λ for b quarks is not well determined.

II. THE SU(3) FLUX-TUBE QUARK MODEL

In this section, we briefly review the potential model of I and discuss the inclusion of one-gluon, short-distance magnetic interactions into it. The basic motivation for the model is quantum chromodynamics, with asymptotically free perturbation theory providing a physical picture for short-distance dynamics and lattice gauge theory as a guide to long-distance, strong-coupling confining dynamics. For example, the potential experienced by a static quark and antiquark held a distance $|\vec{r}|$ apart is assumed to be

$$V_{q\bar{q}}(r) = -\frac{4}{3} \frac{\alpha_c}{|\vec{r}|} + \sqrt{\sigma} |\vec{r}| - M_{q\bar{q}}, \quad (2.1)$$

where $\sqrt{\sigma}$ is the string tension and $M_{q\bar{q}}$ is a constant which sets the zero point in the meson energy spectrum. At short distances, the first term of $V_{q\bar{q}}$ dominates, and its $1/r$ singularity should, in principle, be removed by the vertex factors $\Lambda(r)$. Also the QCD coupling α_c has a weak spatial dependence which we have neglected. In the present work, which focuses on the color-magnetic splittings, we have used Eq. (2.1) from Ref. 1 without any further refinements.

Our extension of Eq. (2.1) to the baryons incorporates the SU(3) character of the gauge fields explicitly. Each of the three quarks in a color-singlet baryon is a source of one unit of flux. At large distances three flux tubes can form, and for SU(3) color they can join at a single point (Fig. 1). Call the positions of the quarks r_i , $i=1,2,3$, and let \vec{r}_4 be the position of the union of the three flux tubes. \vec{r}_4 is determined variationally, i.e., the amount of flux is minimized consistent with Gauss's law and the fixed positions \vec{r}_i . For linear confinement this condition implies that the angles between the flux tubes at their union are each 120° . However, if an interior angle i of the triangle (of quarks) whose vertices (positions) are \vec{r}_i , \vec{r}_j , and \vec{r}_k is greater than 120° , then \vec{r}_4 coincides with \vec{r}_i and the flux configuration degenerates into two linear segments. A natural generalization of Eq. (2.1) to the baryon sector then reads

$$V_{qqq} = -\sum_{i<j\leq 3} \frac{1}{2} \frac{4\alpha_c}{3|\vec{r}_{ij}|} + \sqrt{\sigma} \sum_{i=1,2,3} |\vec{r}_i - \vec{r}_4| - M_{qqq}. \quad (2.2)$$

The first term is the sum of Coulomb-type potentials operative between quark pairs. The factor of $\frac{1}{2}$ is an SU(3) group-theory factor, which occurs because of the color-singlet character of the baryon, and the constant M_{qqq} sets the zero-energy point in the baryon spectrum (it is fit to experiment). The color-electric interactions, Eqs. (2.1) and (2.2), are denoted by V_E in our later discussions.

Finally, the form of the kinetic energies for the quarks must be chosen. In I we used the meson Hamiltonian

$$H_{q\bar{q}} = V_{q\bar{q}} + (\vec{p}_q^2 + m_q^2)^{1/2} + (\vec{p}_{\bar{q}}^2 + m_{\bar{q}}^2)^{1/2} \quad (2.3)$$

in the center of mass $\vec{p}_q + \vec{p}_{\bar{q}} = 0$, and the baryon Hamiltonian was

$$H_{qqq} = V_{qqq} + \sum_{i=1,3} (\vec{p}_i^2 + m_i^2)^{1/2} \quad (2.4)$$

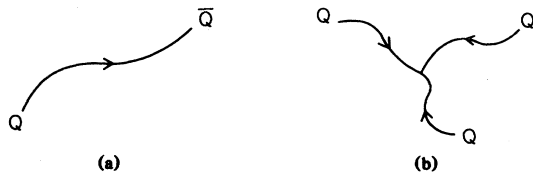


FIG. 1. The flux-tube configurations in (a) mesons and (b) baryons.

in its center of mass $\sum \vec{p}_i = 0$. The masses in both Hamiltonians are the constituent quark masses, but explicit calculation showed that the spin-independent features of the theoretical spectrum of light hadrons are *not* strongly dependent on the choice of the mass.

The spectra of the Hamiltonians [Eqs. (2.3) and (2.4)] can be obtained by variational methods. The specific forms of the kinetic energies in Eqs. (2.3) and (2.4) were motivated in I by considering relativistic-model field theories of confinement. For example, in the Schwinger model (electrodynamics in 1+1 dimensions), Eq. (2.3) is *exact* in the approximation that quark pair production is neglected. In one spatial dimension, Eq. (2.3) is fully relativistic. This gives us confidence that the model's description of radial excitations is sensible.

An analysis⁷ of classical relativistic stringlike solutions of the MIT bag model indicates that orbital excitations may also be described with Eqs. (2.3) and (2.4) with surprisingly good accuracy. Recall how this comes about. Johnson and Thorn⁷ consider the motion of a classical, relativistic mesonic string with light quarks at its ends. The string is pictured as confined flux subject to bag boundary conditions. For purely longitudinal vibrations the system's energy as a function of the distance r between the quarks and their relative momentum p is $E(r,p) = 2p + \sqrt{\sigma}r$ as in the (1+1)-dimensional Schwinger model. Furthermore, the energy of the system as a function of orbital angular momentum J and interquark distance r , $E(J,r)$, can also be computed. To do this one must calculate the angular momentum and energy carried by the flux tube as it rotates. The total angular momentum of the rotating system is $J = J_q + J_f$, where J_q (J_f) is carried by quarks (flux). The total mass of the system consists of three terms $E(J,r) = E_q + E_f + BV$, where E_q (E_f) is the energy of the quarks (flux) and BV is the volume energy associated with the confining pressure B (B is the bag constant and V is the volume of the rotating flux tube in the center of mass). For massless quarks with string ends rotating at the speed of light, Johnson and Thorn find

$$J_q = pr, \quad (2.5)$$

$$J_f = \frac{1}{2} \sqrt{\sigma} r^2 \int_0^1 dv \frac{v^2}{(a-v^2)^{1/2}},$$

where v is the transverse velocity of a bit of rotating string at a distance $r' = rv/2c$ from the center, and

$$E_q(J,r) = 2p = \frac{2J}{r} - \sqrt{\sigma} r \int_0^1 dv \frac{v^2}{(1-v^2)^{1/2}},$$

$$E_f(J,r) = \frac{1}{2} \sqrt{\sigma} r \int_0^1 dv \frac{1+v^2}{(1-v^2)^{1/2}}, \quad (2.6)$$

$$BV = \frac{1}{2} \sqrt{\sigma} r \int_0^1 dv (1-v^2)^{1/2}.$$

So finally,

$$E(J,r) = \frac{2J}{r} + \sqrt{\sigma} r \int_0^1 dv (1-v^2)^{1/2}. \quad (2.7)$$

Since

$$\int_0^1 dv (1-v^2)^{1/2} = \pi/4,$$

the coefficient of the confining potential acting in rotating states differs from that in radially excited states by a factor of $\pi/4 \cong 0.79$. However, if we redo this calculation with the quarks having velocities typical of our bound-state problems for the light mesons, $v \cong 0.7$, then the analysis above goes through with the final replacement $\pi/4 \rightarrow 0.92$. In short, *the same string tension, or linear confining potential, applies to radial and orbital excitations to 10% accuracy*. Although this estimate is model dependent and uses classical notions, it indicates that a potential model picture of the light hadrons should be very good. (As the quark mass increases, the discrepancy 0.92 goes to unity, as expected). Of course, there are additional relativistic (retardation) and field-theoretic (virtual-quark pairs, open channels) effects which this analysis neglects and they could be numerically significant in some cases.

Our light-quark masses will be $m_u = m_d = 360$ MeV, $m_c = 1.84$ GeV, and the bottom-quark mass $m_b = 5.17$ GeV. These values of the light-quark masses give a good account of the color-magnetic interactions and they agree, of course, with past constituent-quark-model work on hadronic matrix elements such as the proton magnetic moment.

Finally, for the sake of completeness, we give expressions for the color-magnetic interaction obtained with the $\exp(-\frac{1}{2}\Lambda^2 q^2)$ vertex form factors. We define $z = r/2\Lambda$ and obtain

$$V_{SS}(q\bar{q}) = \frac{4}{3}\alpha_c \frac{1}{12m^2} \frac{1}{\Lambda^3\sqrt{\pi}} e^{-z^2} \vec{\sigma}_q \cdot \vec{\sigma}_{\bar{q}}, \quad (2.8)$$

$$V_T(q\bar{q}) = \frac{4}{3}\alpha_c \frac{1}{m^2\Lambda^3\sqrt{\pi}} \left[\frac{\sqrt{\pi} \operatorname{erf}(z)}{32z^3} - \left[\frac{1}{24} + \frac{1}{16z^2} \right] e^{-z^2} \right] S_{q\bar{q}}, \quad (2.9)$$

$$V_{SO}^{\text{NR}}(q\bar{q}) = \frac{4}{3}\alpha_c \frac{6}{m^2\Lambda^3\sqrt{\pi}} \left[\frac{\sqrt{\pi} \operatorname{erf}(z)}{32z^3} - \frac{1}{24} e^{-z^2} \right] \vec{L} \cdot \vec{S} \quad (2.10)$$

for heavy quarks. The semirelativistic V_{SO}^{SR} used in light quarks is taken as

$$V_{SO}^{\text{SR}}(q\bar{q}) = x \frac{m}{(m^2 + p^2)^{1/2}} V_{SO}^{\text{NR}}(q\bar{q}). \quad (2.11)$$

In baryons the color-magnetic interaction is given by

$$\sum_{i < j} [V_{SS}(q_i q_j) + V_T(q_i q_j) + V_{SO}(q_i q_j)], \quad (2.12)$$

and the V_{SS} , V_T and V_{SO} between quarks in a baryon are half of those given by Eqs. (2.8)–(2.10) for $q\bar{q}$ pairs.

III. CALCULATIONAL METHODS

The spectra of the heavy $c\bar{c}$ and $b\bar{b}$ mesons are calculated by solving the nonrelativistic Schrödinger equation. The difference

$$2(M^2 + \nabla^2)^{1/2} - 2M + \frac{\nabla^2}{m}$$

is added as a relativistic correction. This correction is quite small (Tables III and IV). The spectra of light mesons and baryons are calculated variationally, by a Monte Carlo method developed to treat light nuclei.⁸ The wave functions are parametrized in the fashion described below, and the expectation values of the semirelativistic Hamiltonian are calculated as described in I, and Ref. 8.

The wave functions of the light mesons are taken to be

$$\psi(nLSJ) = F(r)\phi(nLSJ), \quad (3.1)$$

$$\phi(nLSJ) = r^L R_n(r) \sum_{m_L m_S} \langle JM | L m_L S m_S \rangle \chi_{S m_S} Y_L^{m_L}(\vec{r}), \quad (3.2)$$

$$F(r) = f^c(r) [1 + u^\sigma(r) \vec{\sigma}_q \cdot \vec{\sigma}_{\bar{q}} + u^f(r) \langle S_{q\bar{q}} + 6\vec{L} \cdot \vec{S} \rangle]. \quad (3.3)$$

The $R_n(r)$, $f^c(r)$, $u^\sigma(r)$, and $u^f(r)$ are the variational functions. When ψ has this form, the $u^\sigma(r)$ and $u^f(r)$ are only weakly dependent on $nLSJ$, and the dependence of $R_n(r)$ and $f^c(r)$ on $nLSJ$ is predictable to some extent. Thus the variational calculations of the numerous $nLSJ$ states become simpler.

The function $R_n(r)$ contains the radial nodes of ψ : it is just 1 for $n=0$ states, while it is $1 - \alpha_2 r^2(1 - \alpha_2 r^2 + \alpha_4 r^4)$ for $n=1(2)$ states. The α_i in $R_n(r)$ are determined by requiring that the $\psi(nLSJ)$ is orthogonal to lower energy states having $n' < n$. The central correlation $f^c(r)$ is parametrized as in I:

$$f^c(r) = r^{-\beta} \exp\{-\omega(r)\lambda_1 r - [1 - \omega(r)]\lambda_{1.5} r^{1.5}\}, \quad (3.4)$$

$$\omega(r) = \frac{1 + \exp(-r_0/a)}{1 + \exp((r - r_0)/a)}. \quad (3.5)$$

At short distances ($r \ll r_0$) $f^c(r)$ becomes $r^{-\beta} e^{-\lambda_1 r}$, and the values of β and λ_1 are close to those of the Coulomb wave function.¹ At large distances ($r \gg r_0$), f^c becomes $e^{-\lambda_{1.5} r^{1.5}}$, a form appropriate to a linear potential. β is taken to be nonzero only for the $L=0$ waves. The parameters r_0 and a determine the transition from the Coulomb to linear regions, and it is sufficient to take their values from Ref. 1.

The $u^\sigma(r)$ represents spin-spin correlations. These are treated by the method suggested in Ref. 8:

$$u^\sigma(r) = \beta_\sigma \int \frac{e^{-\mu_\sigma |r-r'|}}{|r-r'|} V_{SS}(r') d^3 r'. \quad (3.6)$$

This correlation is most important for the $L=0$, $S=0$ states, and is necessary to obtain the experimental pion energy.

The $u^f(r)$ represents the influence of the spin-orbit and tensor interactions. The $\langle S_{q\bar{q}} + 6\vec{L} \cdot \vec{S} \rangle$ represents the matrix element in the LSJ state, and the coefficient 6 of the $\vec{L} \cdot \vec{S}$ operator takes into account the larger strength of V_{SO} [compare Eqs. (1.2) and (1.4)]. The function $u^f(r)$ is parametrized as:

$$u^f(r) = \beta_f (1 - e^{-\mu_f r^2}) / r. \quad (3.7)$$

This correlation is most important in 3P_0 states, in which the matrix element $\langle S_{qq} + 6\vec{L} \cdot \vec{S} \rangle$ is -16 . In the 3P_1 and 3P_2 states this matrix element is only -4 and $+5.6$, respectively. The $u^f(r)$ is necessary to obtain the experimental values of the ratios r [Eq. (1.6)] of the energy differences between the 3P_J states of charmonium, etc.

The variational wave function [Eq. (3.1)] does not take into account the mixing between the LSJ and $L'SJ$ states with $L' = L \pm 2$ due to the tensor force. Its effect on $n=0$ states is estimated by diagonalizing the Hamiltonian between LSJ and $L'SJ$ states. It is found to be rather small (≤ 15 MeV); the energy differences between states of different L are larger than the matrix elements of the tensor force.

The variational wave functions for the baryons are very similar to those of I. We take

$$\psi = F_{ijk} \left[\mathcal{S} \prod_{i < j} F_{ij} \right] \phi, \quad (3.8)$$

where ϕ determines the angular momentum, parity, and other quantum numbers of ψ . The ϕ are products of spin, isospin, and r -space states combined to form a symmetric wave function:

$$\phi = \sum \phi(R) \chi(\sigma) \chi(\tau). \quad (3.9)$$

We treat the lowest three spatial states of the qqq system, the 0^+ ground state, the 1^- state, the 0^+ breathing mode. Defining the coordinates $\vec{\rho}$ and $\vec{\lambda}$ as

$$\vec{\rho} = (\vec{r}_1 - \vec{r}_2) / \sqrt{2}, \quad (3.10)$$

$$\vec{\lambda} = (2\vec{r}_3 - \vec{r}_1 - \vec{r}_2) / \sqrt{6}, \quad (3.11)$$

$$\mathcal{S} \prod_{i < j} [1 + u^\sigma(r_{ij}) \vec{\sigma}_i \cdot \vec{\sigma}_j] = 1 + 3u^\sigma(r_{12})u^\sigma(r_{23})u^\sigma(r_{31}) + \sum_{i < j} [u^\sigma(r_{ij}) + u^\sigma(r_{ik})u^\sigma(r_{jk}) - \frac{2}{3}u^\sigma(r_{ij})u^\sigma(r_{jk})u^\sigma(r_{ki})] \vec{\sigma}_i \cdot \vec{\sigma}_j. \quad (3.17)$$

The spin-spin correlations in the baryon have a significant effect on the spectra. They are necessary to obtain experimental N - Δ splitting, etc. On the other hand, most of the effects of the color tensor force on the baryon spectrum

The $\phi(R)$ are, respectively, 1 , $zY_1^m(\vec{z})$, $\vec{z} = \vec{\rho}$ or $\vec{\lambda}$, and $1 - \alpha_2(\vec{\rho}^2 + \vec{\lambda}^2)$ for these three states. The α_2 is determined by requiring that the breathing mode be orthogonal to the ground states.

The eight spin, isospin states are obtained by applying m_S lowering operators to the states:

$$\chi^S(S = \frac{3}{2}, m_S = \frac{3}{2}) = |\uparrow\uparrow\uparrow\rangle, \quad (3.12)$$

$$\chi^\rho(S = \frac{1}{2}, m_S = \frac{1}{2}) = (|\downarrow\uparrow\uparrow\rangle - |\uparrow\downarrow\uparrow\rangle) / \sqrt{2}, \quad (3.13)$$

$$\chi^\lambda(S = \frac{1}{2}, m_S = \frac{1}{2}) = (2|\uparrow\uparrow\downarrow\rangle - |\uparrow\downarrow\uparrow\rangle - |\downarrow\uparrow\uparrow\rangle) / \sqrt{6}. \quad (3.14)$$

The complete ϕ of the eleven baryon states studied in this work are given in Table I.

The pair correlation F_{ij} is taken as

$$F_{ij} = f^c(r) [1 + u^\sigma(r) \vec{\sigma}_i \cdot \vec{\sigma}_j], \quad (3.15)$$

The $u^\sigma(r)$ is parametrized as in Eq. (3.6), and $f^c(r)$ is parametrized as

$$f^c(r) = \exp\{-\omega(r)(\lambda_1 r + \lambda_2 r^2) - [1 - \omega(r)]\lambda_{1.5} r^{1.5}\}. \quad (3.16)$$

The $r^{-\beta}$ term in the $f^c(r)$ of mesons [Eq. (3.4)] is not important for the baryons.¹ It was possible to take all parameters other than $\lambda_{1.5}$ of the $f^c(r)$ from I. The three-body correlation F_{ijk} could also be taken from I.

The spin algebra required to calculate the expectation values of color-magnetic interactions is greatly simplified by noting that the symmetrized product is

TABLE I. Baryon wave functions. A sum over m_L and m_S to obtain the desired J, M state is implied.

$N_{\frac{1}{2}}^+(940)$	$\chi^\lambda(m_S)\chi^\lambda(m_T) + \chi^\rho(m_S)\chi^\rho(m_T)$
$\Delta_{\frac{3}{2}}^+(1230)$	$\chi^S(m_S)\chi^S(m_T)$
$N_{\frac{1}{2}}^-(1520)$	$\chi^\rho(m_T)[\phi^\lambda(m_L)\chi^\rho(m_S) + \phi^\rho(m_L)\chi^\lambda(m_S)]$
$N_{\frac{3}{2}}^-(1535)$	$+\chi^\lambda(m_T)[-\phi^\lambda(m_L)\chi^\lambda(m_S) + \phi^\rho(m_L)\chi^\rho(m_S)]$
$\Delta_{\frac{1}{2}}^-(1650)$	$\chi^S(m_T)[\phi^\lambda(m_L)\chi^\lambda(m_S) + \phi^\rho(m_L)\chi^\rho(m_S)]$
$\Delta_{\frac{3}{2}}^-(1670)$	
$N_{\frac{1}{2}}^-(1650)$	
$N_{\frac{3}{2}}^-(1700)$	$\chi^S(m_S)[\phi^\lambda(m_L)\chi^\lambda(m_T) + \phi^\rho(m_L)\chi^\rho(m_T)]$
$N_{\frac{5}{2}}^-(1670)$	
$N^*\frac{1}{2}(1440)$	$[\chi^\lambda(m_S)\chi^\lambda(m_T) + \chi^\rho(m_S)\chi^\rho(m_T)][1 - \alpha(\rho^2 + \lambda^2)]$
$\Delta^*\frac{3}{2}(1700)$	$\chi^S(m_S)\chi^S(m_T)[1 - \alpha(\rho^2 + \lambda^2)].$

TABLE II. Expectation values of various terms in the Hamiltonian (MeV), and the rms radii (fm) for light mesons. The V_L and V_C denote the linear and Coulomb parts of the color-electric interaction in mesons.

$nLSJ^\pi$	E	$2(m^2+p_1^2)^{1/2}$	V_L	V_C	V_{SS}	V_T	V_{SO}	$\langle r^2 \rangle^{1/2}$
0000 ⁻	140	1948	278	-525	-811	0	0	0.16
0011 ⁻	751	1066	592	-222	65	0	0	0.32
0101 ⁺	1113	1486	683	-184	-122	0	0	0.38
0110 ⁺	931	1502	659	-182	36	-131	-203	0.36
0111 ⁺	1180	1291	795	-147	16	48	-73	0.43
0112 ⁺	1256	1210	870	-130	8	-8	56	0.46
1000 ⁻	1114	1489	765	-210	-180	0	0	0.41
1011 ⁻	1442	1375	931	-186	72	0	0	0.53
0202 ⁻	1560	1434	1000	-112	-12	0	0	0.53
0211 ⁻	1441	1593	882	-129	+8	-37	-126	0.47
0212 ⁻	1567	1434	995	-112	+4	25	-29	0.53
0213 ⁻	1620	1337	1091	-100	+1	-6	47	0.57
0303 ⁺	1892	1588	1148	-93	-1	0	0	0.60
0312 ⁺	1816	1694	1066	-102	+1	-16	-77	0.56
0313 ⁺	1894	1588	1148	-93	0	+16	-15	0.60
0314 ⁺	1933	1495	1241	-86	0	-4	+37	0.64
2011 ⁻	1957	1506	1294	-142	49	0	0	0.72
0404 ⁻	2177	1680	1327	-80	0	0	0	0.69
0413 ⁻	2125	1752	1265	-84	0	-8	-50	0.66
0414 ⁻	2178	1680	1327	-80	0	+10	-9	0.69
0415 ⁻	2207	1651	1355	-78	0	-3	32	0.70
0505 ⁺	2438	1756	1501	-70	0	0	0	0.77
0514 ⁺	2398	1806	1454	-72	0	-5	-35	0.75
0515 ⁺	2438	1756	1501	-70	0	+6	-5	0.77
0516 ⁺	2462	1756	1501	-70	0	-2	27	0.77

are estimated by diagonalizing the 2×2 Hamiltonian matrix for the P -wave baryons having $S = \frac{1}{2}$ and $\frac{3}{2}$.

IV. RESULTS

The calculated expectation values of the kinetic energy and central, V_{SS} , V_T , and V_{SO} potentials etc., are given in Tables II–V. The calculated values of the root-mean-square radii can also be found in these tables. In this section we discuss some of the interesting results of these calculations, and compare the energies with experiment.

The wave functions used in I do not have the spin correlations $u^g(r)$ and $u^f(r)$. Using those wave functions corresponds to treating the color-magnetic interaction in first-order perturbation theory. In Table VI, we compare the energies of some of the states in this first-order calculation, and in the variational calculation using the wave functions given in the last section. We find that the first-order calculation is not valid for the states in which the color-magnetic interaction is very attractive. The radii of these states change because of the increased binding, and that effect results in even more attraction from the color-

TABLE III. Same as Table II, for baryons. V_L^{2B} and V_L^{3B} denote the two- and three-body parts of the linear potential in the baryons as defined in I.

State	E	$\sum_i (m^2 + p_i^2)$	V_L^{2B}	V_L^{3B}	V_C	V_{SS}	V_T	V_{SO}	$\langle r^2 \rangle^{1/2}$
$N_{\frac{1}{2}}^+$	940	2025	761	69	-404	-252	0	0	0.32
$\Delta_{\frac{3}{2}}^+$	1240	1712	925	91	-298	68	0	0	0.39
$N_{\frac{1}{2}}^-$	1399	2080	989	88	-305	-162	0	-32	0.42
$N_{\frac{3}{2}}^-$	1446	2086	988	86	-306	-165	0	+16	0.42
$\Delta_{\frac{1}{2}}^-$	1566	1975	1036	100	-269	-17	0	-2	0.43
$\Delta_{\frac{3}{2}}^-$	1564	1959	1043	101	-266	-15	0	+1	0.44
$N_{\frac{1}{2}}^-$	1514	1936	1061	101	-264	51	-33	-79	0.44
$N_{\frac{3}{2}}^-$	1628	1948	1057	99	-265	51	+27	-32	0.44
$N_{\frac{5}{2}}^-$	1661	1886	1097	106	-248	40	-6	+44	0.44
$N_{\frac{1}{2}}^+$	1583	2007	1179	104	-303	-147	0	0	0.51
$\Delta_{\frac{3}{2}}^+$	1847	2047	1159	107	-299	+91	0	0	0.51

TABLE IV. Same as Table II, for charmonium.

$nLSJ^\pi$	E	$2 \left[m_i + \frac{p_i^2}{2m} \right]$	$2(m_i^2 + p_i^2)^{1/2}$	V_L	V_C	V_{SS}	V_T	V_{SO}	$\langle r^2 \rangle^{1/2}$
0000 ⁻	2978	4158	4103	301	-466	-87	0	0	0.17
0011 ⁻	3097	4025	3998	344	-389	18	0	0	0.19
0101 ⁺	3513	4067	4041	556	-207	-3	0	0	0.30
0110 ⁺	3412	4179	4133	497	-239	2	-24	-84	0.27
0111 ⁺	3494	4084	4056	545	-212	1	9	-29	0.29
0112 ⁺	3543	4037	4015	578	-197	1	-1	+22	0.31
1000 ⁻	3615	4176	4114	664	-248	-41	0	0	0.36
1011 ⁻	3681	4129	4083	691	-231	+11	0	0	0.38
0211 ⁻	3772	4161	4124	709	-155	0	-3	-30	0.37
2000 ⁻	4050	4274	4195	946	-187	-31	0	0	0.52
2011 ⁻	4100	4143	4178	967	-179	+9	0	0	0.53
1211 ⁻	4150	4277	4214	972	-129	0	-3	-29	0.52
3011 ⁻	4454	4351	4264	1207	-152	7	0	0	0.66

magnetic interaction. A similar effect is seen in bag-model calculations,⁹ in which the pion bag radius decreases because of the attractive one-gluon-exchange interaction.

The spectra of isospin $T=1$ mesons with $L=0$ and $L \geq 1$ is compared with experiment in Figs. 2 and 3. In general the calculated energies are a few percent lower than the experimental energies. We believe that better agreement with experiment will be obtained with a little larger value of α_c . However if the ρ' (1250 MeV) state is confirmed, in future experiments, it would be difficult to simultaneously explain the large π - ρ splitting, and the near degeneracy of π' and ρ' in the constituent quark model.

The baryon spectra obtained with the V_E and $V_E + V_{SS}$ are compared with experiment in Fig. 4. The calculated energy of the Roper resonance is too high, and the P -wave baryons are a little too low. The theoretical Roper would move higher up if the α_c is increased to better reproduce the meson spectrum. The calculated spectra of P -wave baryons with V_T and $V_T + V_{SO}$ are compared with experiment in Fig. 5. The observed $S = \frac{1}{2}$, $J^\pi = \frac{1}{2}^-$, and $\frac{3}{2}^-$ N (and Δ) states are nearly degenerate, and the splitting of the $S = \frac{3}{2}$, $J^\pi = \frac{1}{2}^-$, $\frac{3}{2}^-$, and $\frac{5}{2}^-$ states is well reproduced

by V_T only. From Fig. 5 one would surmise that the V_{SO} in qqq is almost zero and the V_{SS} of the present model is giving $\sim 25\%$ too large splitting between the $S = \frac{1}{2}$ and $\frac{3}{2}$ nucleon states.

It is interesting to consider the mixing caused by the tensor force Eq. (1.2) between various P -wave baryon states. The wave functions of the $N^*(J^\pi = \frac{1}{2}^-, 1530)$ and $N^*(J^\pi = \frac{3}{2}^-, 1520)$ are found to be

$$|N^*(1530)\rangle = 0.986 \left| \frac{1}{2} \frac{1}{2} \right\rangle + 0.168 \left| \frac{3}{2} \frac{1}{2} \right\rangle, \quad (4.1)$$

$$|N^*(1520)\rangle = 0.999 \left| \frac{1}{2} \frac{3}{2} \right\rangle - 0.04 \left| \frac{3}{2} \frac{3}{2} \right\rangle, \quad (4.2)$$

where the kets are labeled with S and J . These wave functions are significantly different from those obtained by Hey, Litchfield, and Cashmore¹⁰ by fitting experimental decay rates. The wave functions of Ref. 10 are

$$|N^*(1530)\rangle = 0.85 \left| \frac{1}{2} \frac{1}{2} \right\rangle + 0.53 \left| \frac{3}{2} \frac{1}{2} \right\rangle, \quad (4.3)$$

$$|N^*(1520)\rangle = 0.98 \left| \frac{1}{2} \frac{3}{2} \right\rangle - 0.18 \left| \frac{3}{2} \frac{3}{2} \right\rangle. \quad (4.4)$$

It has been shown by Isgur and Karl¹¹ that the wave functions of Ref. 10 can be reproduced by (i) treating color-magnetic interactions in first-order perturbation theory,

TABLE V. Same as Table II, for b -quarkonium.

$nLSJ^\pi$	E	$\sum_i \left[m + \frac{p_i^2}{2m} \right]$	$2(m_i^2 + p_i^2)^{1/2}$	V_L	V_C	V_{SS}	V_T	V_{SO}	$\langle r^2 \rangle^{1/2}$
0000 ⁻	9372	10844	10809	180	-677	-65	0	0	0.10
0011 ⁻	9460	10711	10697	201	-577	13	0	0	0.11
0110 ⁺	9837	10716	10704	342	-291	0	-10	-33	0.18
0111 ⁺	9869	10667	10659	362	-270	0	4	-12	0.19
0112 ⁺	9888	10642	10636	375	-258	0	-1	+10	0.20
1000 ⁻	9949	10742	10720	442	-314	-26	0	0	0.24
1011 ⁻	9983	10707	10691	456	-295	6	0	0	0.25
1110 ⁺	10191	10770	10752	558	-211	0	-8	-27	0.30
1111 ⁺	10217	10737	10723	575	-199	0	3	-10	0.31
1112 ⁺	10234	10718	10706	587	-191	0	-1	+8	0.32
2011 ⁻	10320	10772	10752	658	-221	5	0	0	0.36
3011 ⁻	10595	10843	10818	832	-184	4	0	0	0.45

TABLE VI. Nonperturbative effects of color-magnetic interaction.

State	Zeroth order		First order E (MeV)	Variational	
	E (MeV)	R_{rms} (fm)		E (MeV)	R_{rms} (fm)
π	671	0.29	373	140	0.16
ρ	671	0.29	770	750	0.32
N	1141	0.36	1031	940	0.32
Δ	1141	0.36	1251	1240	0.39
δ	1202	0.43	990	931	0.36
A_1	1202	0.43	1180	1179	0.43
A_2	1202	0.43	1258	1256	0.46
$c\bar{c}({}^3P_0)$	3518	0.30	3450	3412	0.27
$c\bar{c}({}^3P_1)$	3518	0.30	3500	3494	0.29
$c\bar{c}({}^3P_2)$	3518	0.30	3543	3543	0.31

(ii) neglecting $\vec{L}\cdot\vec{S}$ interaction, and (iii) using harmonic-oscillator wave functions.

The tensor force mixes the $S=\frac{1}{2}$ and $\frac{3}{2}$ states, and if we take the results of Ref. 10 seriously we must conclude

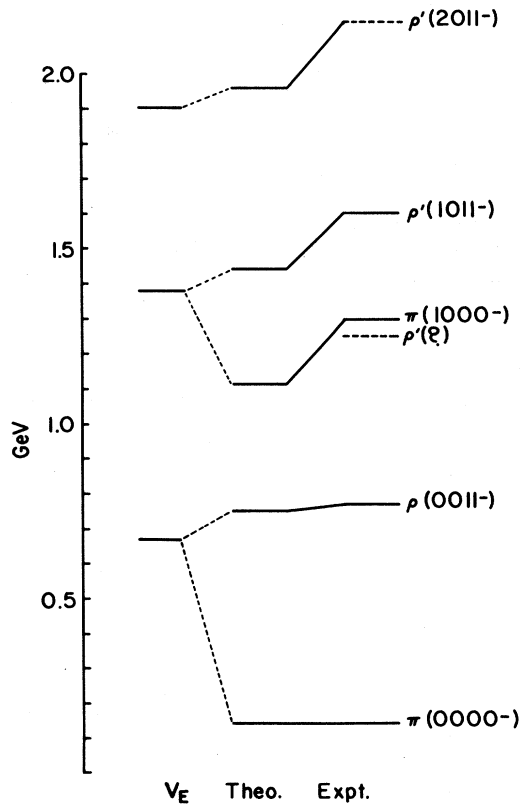


FIG. 2. The spectrum of $L=0$ mesons. The first two columns give the spectra calculated with V_E only and with $V_E+V_{SS}+V_T+V_{SO}^{SR}$, respectively. The semirelativistic V_{SO}^{SR} of Eq. (2.11) with $\alpha=0.7$ is used in these calculations. The third column gives the experimental spectrum of isospin $T=1$ mesons from Ref. 6. Uncertain levels, found only in the meson data card, are shown by dashed lines. All known $T=1, J^\pi=0^-$ and 1^- levels are included in the figure; and the $nLSJ^\pi$ assignments are given in parentheses.

that the tensor force in our model is too weak. However, if we phenomenologically increase the strength of the tensor force we will severely overestimate the splitting of P -wave baryon energies. The true baryon states are certainly much more complex than those suggested by Eqs. (4.1)–(4.4). They have meson clouds which perhaps influence the mixings.

The calculated spectrum of charmonium shown in Fig. 6 is in good agreement with experiment. The splittings of the 3P_J states is well reproduced, and the main problem appears to be that the energy of $n=2$ 3S_1 state is too high. The calculated $b\bar{b}$ spectrum shown in Fig. 7 is also in reasonable agreement with experiment.

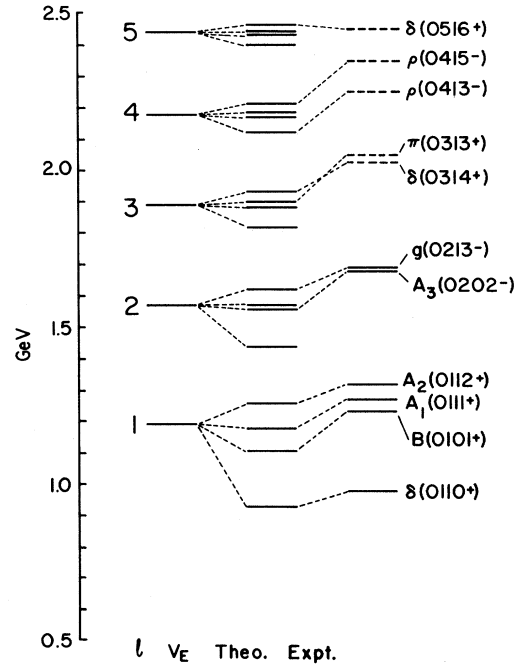


FIG. 3. The orbital-excitation spectrum of mesons. See caption of Fig. 1 for notation. All known $T=1, J^\pi \neq 0^-$ and 1^- states, except for the $2^- \pi(2100)$ states, are shown in the figure. The $\pi(2100)$ is an "uncertain" state, and it may be a radial excitation of the $A_3(1680)$.

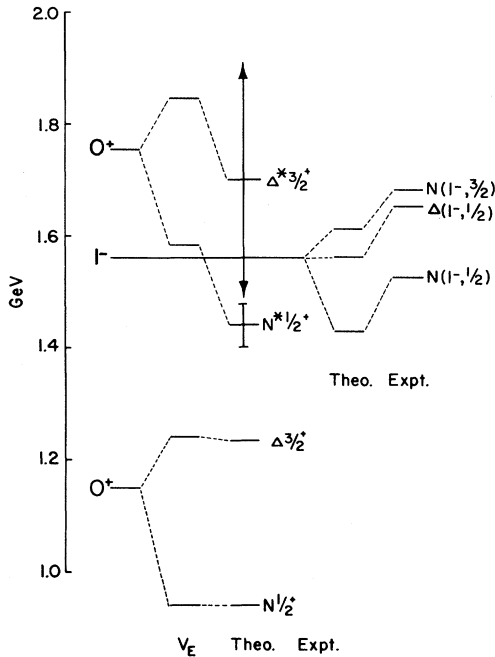


FIG. 4. The baryon spectrum. The first column gives the color-electric spectrum labeled by L^π , the next gives the $L^\pi=0^+$ baryon energies calculated with $V_E + V_{SS}$. The third column gives the experimental energies of these states; the large uncertainties in the $N^*(\frac{1}{2}^+)$ and $\Delta^*(\frac{3}{2}^+)$ are indicated by error bars. The calculated energies of the $L^\pi=1^-$ baryons with $V_E + V_{SS}$ interaction are given in fourth column. The experimental energies shown in the last column are the centroids of the $J = |L - S|$ to $L + S$ states.

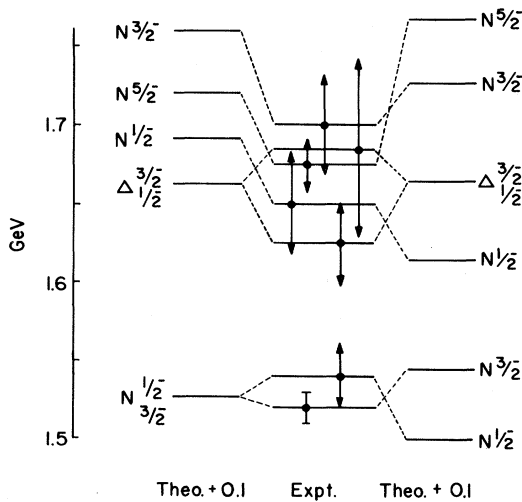


FIG. 5. The spectra of P -wave baryons. The first column gives the spectrum calculated with $V_E + V_{SS} + V_T$, the second gives the experimental spectrum with the error bars, and third gives the spectrum calculated with $V_E + V_{SS} + V_T + V_{SO}$. The semirelativistic V_{SO}^{SR} with $x=0.7$ is used in these calculations. A constant 0.1 GeV is added to all calculated energies to facilitate comparison with experiment.

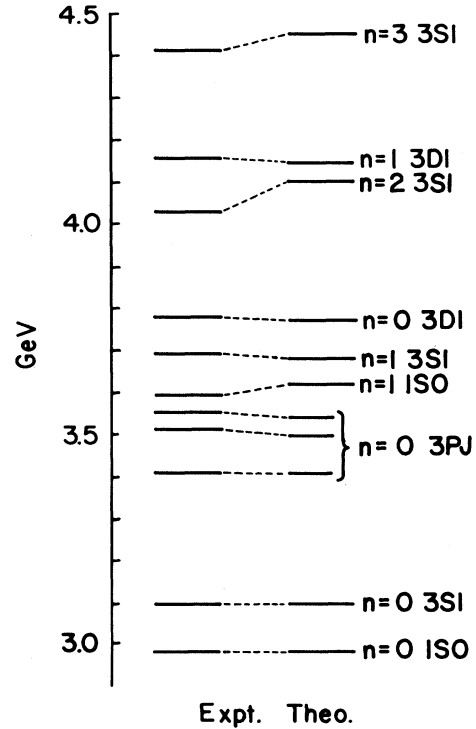


FIG. 6. The experimental and calculated spectrum of charmonium with $V_E + V_{SS} + V_T + V_{SO}^{NR}$. The experimental energies are from Ref. 6.

The values of the constants $M_{q\bar{q}}$, $M_{c\bar{c}}$, $M_{b\bar{b}}$, and M_{qqq} are given in Table VII. It should be possible to make slight changes in the assumed masses of m_c and m_b and make

$$M_{q\bar{q}} = M_{c\bar{c}} = M_{b\bar{b}} \quad (4.5)$$

However, there is no fundamental understanding of these

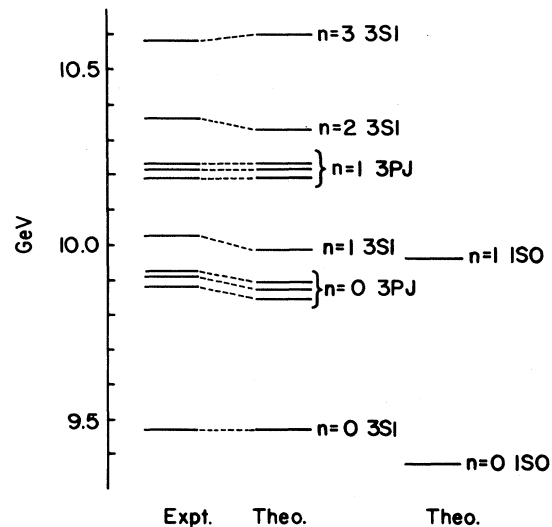


FIG. 7. The experimental and calculated spectrum of $b\bar{b}$ with $V_E + V_{SS} + V_T + V_{LS}$ (nonrelativistic). The experimental energies are taken from a compilation of Moxhay and Rosner (Ref. 12).

TABLE VII. The energy constants in GeV.

$M_{q\bar{q}}$	0.75
$M_{c\tau}$	0.87
$M_{b\bar{b}}$	0.87
M_{qqq}	1.27

numbers. Curiously,

$$M_{qqq} \sim \frac{3}{2} M_{q\bar{q}}. \quad (4.6)$$

V. CONCLUSIONS

The constituent quark model, with its rather simple Hamiltonian with very few parameters, does seem to give a semiquantitative description of the number of spectra considered in this work. The two main failures of the model in the context of spectroscopy, are (i) generally the spacing between radial excitations is a bit larger, while that between rotational excitations is a little smaller than experiment, and (ii) the model predicts spin-orbit splitting

that is not observed in P -wave baryons. In light of the Johnson and Thorn model⁷ of rotating flux tubes, one could have expected the opposite of our problem (i). That model would suggest that if the string tension is adjusted to reproduce radial excitations, the splittings between rotational states would be too large in a potential model which neglects the angular momentum carried by the flux tube.

The model also fails to reproduce the experimental charge radii of the nucleon and pion. This problem is certainly due to the neglect of pair production terms in our Hamiltonian. Such terms would give rise to experimentally observed couplings $N \rightarrow N + \pi$, $\Delta + \pi$, $\rho \rightarrow 2\pi$, etc. These couplings will also affect the spectrum, and may be necessary to obtain a more accurate description of the hadron spectroscopy.

ACKNOWLEDGMENTS

This work was supported by the National Science Foundation under Grants Nos. NSF PHY81-21399 and NSF PHY82-01948. The authors thank J. Rosner for conversations and suggestions.

¹J. Carlson, J. Kogut, and V. R. Pandharipande, Phys. Rev. D **27**, 233 (1983).
²A. De Rújula, Howard Georgi, and S. L. Glashow, Phys. Rev. D **12**, 147 (1975).
³Nathan Isgur and Gabriel Karl, Phys. Rev. D **18**, 4186 (1978); **19**, 2653 (1979); **20**, 1191 (1979).
⁴H. R. Fiebig and B. Schwesinger, SUNY report, 1982 (unpublished).
⁵R. P. Feynman, R. D. Field, and G. C. Fox, Phys. Rev. D **18**, 3320 (1978).

⁶Particle Data Group, Phys. Lett. **111B**, 1 (1982).

⁷K. Johnson and C. B. Thorn, Phys. Rev. D **13**, 1934 (1976).

⁸J. Carlson and V. R. Pandharipande, Nucl. Phys. **A371**, 301 (1981).

⁹C. E. Carlson, T. H. Hansson, and C. Peterson, Phys. Rev. D **27**, 1556 (1983).

¹⁰A. J. G. Hey, P. J. Litchfield, and R. J. Cashmore, Nucl. Phys. **B95**, 516 (1975).

¹¹N. Isgur and Gabriel Karl, Phys. Lett. **72B**, 109 (1977).

¹²P. Moxhay and J. L. Rosner, Phys. Rev. D **28**, 1132 (1983).